ARTICLE

doi:10.1038/nature11298

Parity–time synthetic photonic lattices

Alois Regensburger[1,2], Christoph Bersch[1,2], Mohammad-Ali Miri[3], Georgy Onishchukov[2], Demetrios N. Christodoulides[3] & Ulf Peschel[1]

The development of new artificial structures and materials is today one of the major research challenges in optics. In most studies so far, the design of such structures has been based on the judicious manipulation of their refractive index properties. Recently, the prospect of simultaneously using gain and loss was suggested as a new way of achieving optical behaviour that is at present unattainable with standard arrangements. What facilitated these quests is the recently developed notion of 'parity–time symmetry' in optical systems, which allows a controlled interplay between gain and loss. Here we report the experimental observation of light transport in large-scale temporal lattices that are parity–time symmetric. In addition, we demonstrate that periodic structures respecting this symmetry can act as unidirectional invisible media when operated near their exceptional points. Our experimental results represent a step in the application of concepts from parity–time symmetry to a new generation of multifunctional optical devices and networks.

In designing an optical system, nature demands that only a few basic 'ingredients' be used: refractive index, gain and loss. There is no doubt as to how useful index contrast is in controlling optical dynamics. Shaping the refractive index profile has led to unprecedented advancements in optics ranging from the design and fabrication of photonic crystals[1] and photonic crystal fibres[2] to the exploration of nanoplasmonics[3–6] and negative-index metamaterials[7]. Loss is abundant in physical systems, but is typically considered a problem. Gain, however, as afforded by lasers, is valuable in optoelectronics because it provides a means to induce lasing or to overcome losses[4–6]. The question naturally arises as to whether new artificial optical structures and materials can be synthesized by mixing together these three ingredients in roughly comparable proportions, and, if so, how this can be done without running into uncontrollably growing or decaying optical modes. The answer may come from some recent abstract developments in quantum field theories.

In 1998, it was shown that a wide class of non-Hermitian Hamiltonians can actually possess entirely real spectra as long as they respect parity–time symmetry[8]. This is clearly counterintuitive given the fact that this symmetry is commonly associated with purely Hermitian systems. In quantum mechanics, the action of the parity operator $\hat{P}$ is defined by the relations $\hat{x}\rightarrow-\hat{x}$ and $\hat{p}\rightarrow-\hat{p}$, and that of the $\hat{T}$ operator leads to $\hat{p}\rightarrow-\hat{p}$, $i\rightarrow-i$ and $\hat{x}\rightarrow\hat{x}$, where $\hat{x}$ and $\hat{p}$ represent the position and momentum operators, respectively. In general, a Hamiltonian $\hat{H}=\hat{p}^2/2+V(\hat{x})$ associated with a complex potential $V(\hat{x})$ is parity–time symmetric provided that it commutes with the parity–time operator. In this case, $\hat{H}\hat{P}\hat{T}=\hat{P}\hat{T}\hat{H}$ and, thus, $\hat{H}$ and $\hat{P}\hat{T}$ may share a common set of eigenfunctions[8–14].

Given that the evolution of the system is described by a Schrödinger evolution equation of the form $i\Psi_t=\hat{H}\Psi$, where Ψ_t denotes the partial derivative of Ψ with respect to time, it can be shown[9] that a necessary (but not sufficient) condition for this to occur is that the complex potential involved in such a Hamiltonian satisfies $V(x)=V^*(-x)$. This implies that the real part of the potential must be an even function of position and that the imaginary part must be odd. In such pseudo-Hermitian configurations, the eigenfunctions are no longer orthogonal and, hence, the vector space of eigenmodes is skewed[8,10]. Even more intriguing is the possibility of a sharp, symmetry-breaking transition once a non-hermiticity parameter exceeds a certain critical value, the 'parity–time threshold'. In such a regime, the Hamiltonian and the parity–time operator no longer have the same set of eigenfunctions (even though they commute) and as a result the eigenvalues of the system cease to be all real. In addition, this broken parity–time symmetry phase is associated with the appearance of exceptional points[8–11], where the eigenvalue branches merge and parity–time symmetry breaks down.

Although the ramifications of these developments are still a matter of debate within the framework of theoretical physics, it has recently been recognized that optics can provide a productive test bed where the notions of parity–time symmetry can be experimentally explored, and ultimately used[15–17]. Given that such photonic systems are entirely classical, they can be fully realized without introducing any conflict with the hermiticity of quantum mechanics. In optics, a complex potential can be readily built by judiciously incorporating, in a balanced way, regions having optical gain and loss[15]. What allows this duality between quantum mechanics and optics is the isomorphic nature of the wave equations involved (Supplementary Methods, section 1.9). In this case, the complex refractive index plays the part of a potential and 'parity–time symmetry', hereafter PT symmetry in the context of optics, therefore demands[15–17] that $n(x)=n^*(-x)$. However, so far, the realization of structures that simultaneously exhibit a symmetric refractive index distribution and an antisymmetric gain/loss profile has been hampered by technical difficulties. As a result, PT symmetry has been observed only in elemental two-component systems[18–21]. It will be important to devise new, versatile platforms where such phenomena can be explored. If successful, a new generation of optical devices, materials and networks may result, including, for example, unidirectional on-chip devices[22] as well as PT-symmetric, high-power laser systems and laser oscillators[23–31]. Finally, ideas from PT symmetry may provide a viable route to overcoming losses that have so far hindered progress in other areas of applied physics such as plasmonics and metamaterials[5–7].

In this Article, we report the experimental demonstration of temporally resolved optical beam dynamics in large-scale, PT-symmetric lattices. The unusual band structure associated with such extended systems is probed along with power unfolding and secondary emissions resulting from the skewed character of the Floquet–Bloch modes. In addition, we observe the unidirectional invisibility of a

[1]Institute of Optics, Information and Photonics, University of Erlangen-Nürnberg, Staudtstraße 7/B2, 91058 Erlangen, Germany. [2]Max Planck Institute for the Science of Light, Günther-Scharowsky-Straße 1, Bau 24, 91058 Erlangen, Germany. [3]CREOL, College of Optics and Photonics, University of Central Florida, Orlando, Florida 32816–2700, USA.

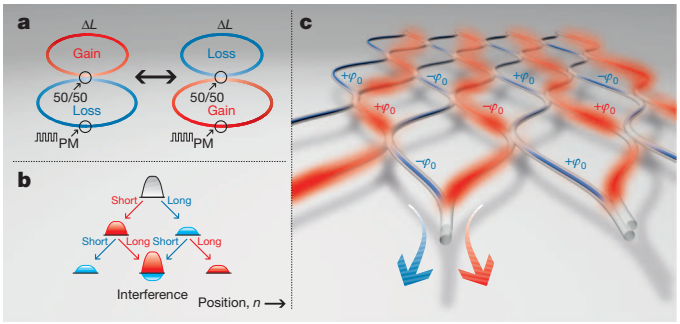

Figure 1 | PT-symmetric fibre networks. **a**, Two coupled fibre loops periodically switching between gain and loss as used in the experiment (Supplementary Fig. 1). Pulses are delayed or advanced as a result of a length difference ΔL between the loops. PM, phase modulator. **b**, Pulse evolution in the networks. Passages through short and long loops are indicated. **c**, Equivalent PT-symmetric lattice network. Gain (red) and loss (blue) channels are positioned antisymmetrically and are periodically coupled. Moreover, the real part of the potential is evenly imposed by phase shifts $\pm\varphi_0$.

PT-symmetric temporal grating when operating close to the system's exceptional points. Such structures have no effect on transmitted light, and their reflectivity greatly varies with the direction of propagation. The underlying flexibility of the arrangements proposed can be used to implement a diverse family of 'PT synthetic' structures and networks with altogether new properties and functionalities.

In our experiments, large-scale, PT-symmetric optical networks are realized in the temporal domain. This is accomplished by shaping the evolution of a sequence of pulses in two appropriately designed fibre loops connected by a 50/50 coupler (Fig. 1a and Supplementary Methods, section 1). A length differential ΔL between the two pathways leads to discretized arrival times for the optical pulses and to a transverse coupling between neighbouring time slots. The induced transverse pulse transport[32,33] can be directly observed by monitoring the output of tap nodes. A pulse traversing the short loop will be advanced, whereas pulses propagating along the long loop will be temporally delayed. The resulting pulse trains emerging from the short and long loops eventually interfere at the coupler in a manner depending on the phases acquired along their respective pathways (Fig. 1b and Supplementary Methods).

In this system, PT symmetry is imposed by temporally alternating gain and loss in the two loops by means of optical amplifiers in conjunction with amplitude modulators. In addition, the even, real part of the optical PT potential ($\mathrm{Re}\{n(x)\}$) can be discretely introduced using phase modulation. The PT nature of this configuration becomes apparent by considering the fully equivalent spatial waveguide network shown in Fig. 1c, where the time slots associated with the set-up described here are mapped on discrete transverse sites n. A pulse delay or advancement in the temporal domain corresponds to a transition towards the left or the right in the spatial network of Fig. 1c. The light evolution in these spatiotemporal lattices is described by the following recursion equations[33]:

$$u_n^{m+1} = \frac{G^{\pm 1/2}}{\sqrt{2}}(u_{n+1}^m + iv_{n+1}^m)$$
$$v_n^{m+1} = \frac{G^{\mp 1/2}}{\sqrt{2}}(iu_{n-1}^m + v_{n-1}^m)e^{i\varphi(n)} \quad (1)$$

In the temporal domain, u_n^m and v_n^m denote the amplitudes of a sequence of pulses occupying time slots n within the short and long loop, respectively, after the mth round trip. The phase function $\varphi(n)$ provides the symmetric, real part of the PT potential, by imposing a phase $\pm\varphi_0$ on the pulses, and the antisymmetric, imaginary component of the effective potential is induced by a gain/loss factor G. In equation (1), the exponent of G switches from $-1/2$ to $+1/2$ between alternate loops in every step m; that is, the loops are repeatedly switched between gain and loss in equal amounts.

Our experimental set-up (Fig. 1a), as well as its equivalent optical network (Fig. 1c), are periodic in both m and n, thus leading to a band

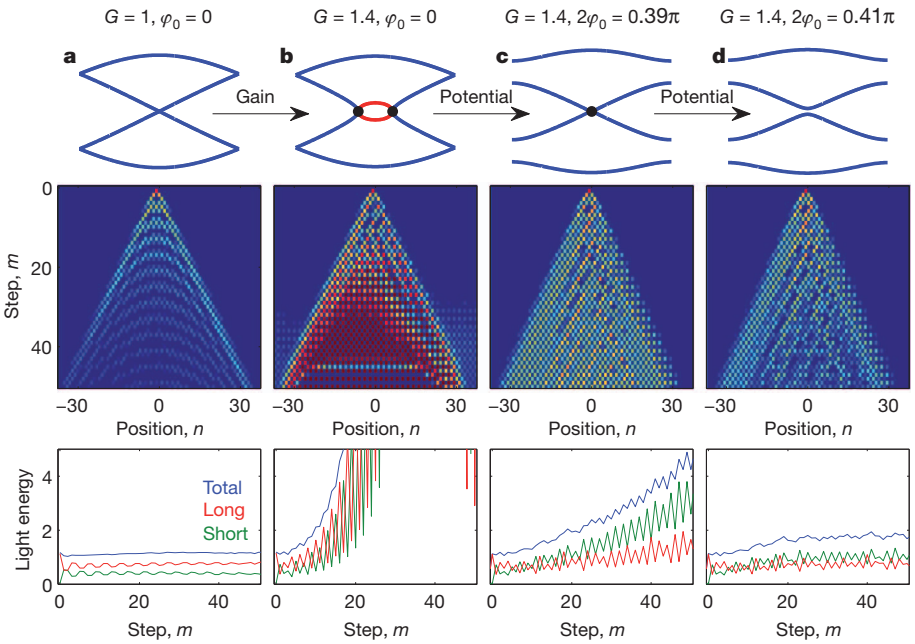

Figure 2 | Band structure and measured single-pulse evolution in the PT synthetic network. **a**, Passive system ($G = 1$) without phase potential ($\varphi_0 = 0$) with an entirely real (blue) band structure and no band gaps. The evolution of a pulse injected into the long loop is similar[33] to a quantum walk[32]. Measured pulse intensities at position n and step (loop round trip) m are indicated in the logarithmic colour scale: red, high intensity (1); dark blue, low intensity ($10^{-2.05}$). **b**, Same as **a**, but with net gain/loss ($G = 1.4$). Parts of the band structure become imaginary (red), leading to an exponential energy growth. Black points in the figures denote exceptional points. **c**, Same as **b**, but with a phase potential ($2\varphi_0 = 0.39\pi$) partly stabilizing the system, leading to a linear growth in energy. **d**, A further increase of the real-valued potential ($2\varphi_0 = 0.41\pi$) opens a band gap, making the band structure again entirely real. Power unfolding is observed in this case; that is, the optical energy is no longer conserved but oscillates about a mean value because the eigenmodes are not orthogonal. For data in both loops, colour scales and a comparison with simulations, see Supplementary Figs 4 and 5.

structure as shown in Fig. 2 (see Supplementary Fig. 6 for details). In fact, all the unusual dynamics in these PT synthetic networks can be traced back to their peculiar band features. As Fig. 2 indicates, the bands can show new characteristics including the formation of exceptional points and the possibility of band-merging effects[15,17]—both a direct outcome of a spontaneously broken PT symmetry. In the passive case, when the imaginary part of the potential is absent[33], two bands form without a gap (Fig. 2a), and the system hence has no PT threshold. Therefore, even a small amount of gain/loss G abruptly forces the bands to merge at the exceptional points, where a transition to imaginary eigenvalues occurs (Fig. 2b). To establish a finite threshold, a symmetric phase potential $\varphi(n)$ has to be introduced into the time lattice. The presence of such a potential forces the bands apart, thus creating a band gap. In this arrangement, the spectrum is again entirely real, in spite of the fact that the system is not Hermitian (Fig. 2d).

In the experiment, we probe the entire band structure of this lattice by simultaneously exciting all bands with a single pulse. Although power is conserved in the passive time lattice (Fig. 2a), exponential growth occurs (Fig. 2b) above the point at which PT symmetry is broken, where the spectrum ceases to be real. However, if the system is operated at threshold, with only exceptional points present (Fig. 2b, c, black points), the power increases linearly in time as clearly shown in Fig. 2c, in agreement with previous theoretical predictions[34–36]. Even below the symmetry-breaking point, power oscillations are observed (Fig. 2d). The question is why this occurs, given that the bands are entirely real. The answer has to do with the very fact that the network's Floquet–Bloch modes are no longer orthogonal and, consequently, power 'hidden' in the system can reappear during evolution[15,35]. As a result, the total power in the system undergoes oscillations because of mode interference effects.

The versatility of the time-multiplexed lattice described here allows us to explore further the onset of PT symmetry breaking by performing a parameter scan throughout the accessible range of the phase potential φ_0 and gain/loss coefficient G (Fig. 3a). As Fig. 3a shows, if the phase modulation is strong enough we observe a harmonic coexistence between gain and loss (blue region) that can be suddenly broken by small parameter variations (as in the red area), resulting in an exponential energy rise as shown in Fig. 3b. However, in the exact PT phase the power oscillates during evolution (Fig. 3c). As both gain/loss G and the phase potential $\varphi(n)$ can be dynamically changed during the course of light propagation, it is possible to implement abrupt and gradual transitions from PT-symmetric to passive regimes in our temporal photonic lattice. Moreover, the sharp transitions between these phases can provide a precise mechanism for dynamic power control in laser cavities. Given the conceptual similarity of our set-up (Fig. 1a) to figure-eight fibre lasers, it might be possible to apply our modulation schemes (Supplementary Fig. 3) to achieve enhanced pulse control. For example, for the phase in which PT symmetry is broken, pulse trains with a fixed phase relation and a spacing defined by the path difference and not the total length of the loops could be produced.

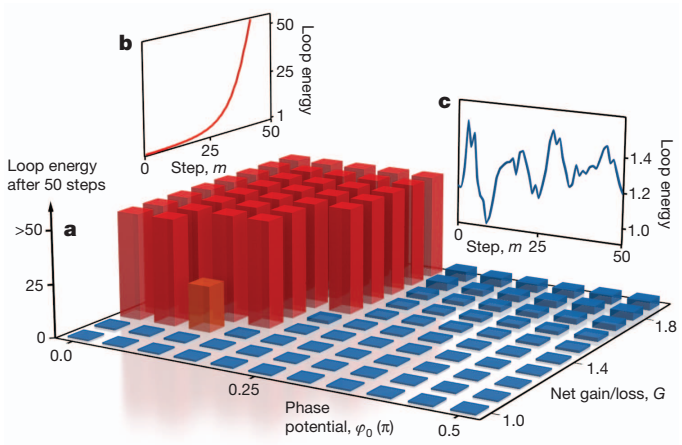

Figure 3 | Exploring the PT threshold of a lattice using a two-parameter scan. a, Total energy experimentally observed after 50 round trips m. A wide range of accessible parameters corresponding to the linear potential φ_0 and the magnitude of gain/loss G is experimentally searched, revealing the PT phase transition boundary, within which a sudden jump in energy occurs (red region). The small energy increase observed outside this region is caused by experimental imperfections and power unfolding. **b**, **c**, Observed evolution in the total energy of the system for partly complex (**b**; see Fig. 2b) and entirely real (**c**; see Fig. 2d) lattice spectra: unlimited exponential growth versus power oscillations.

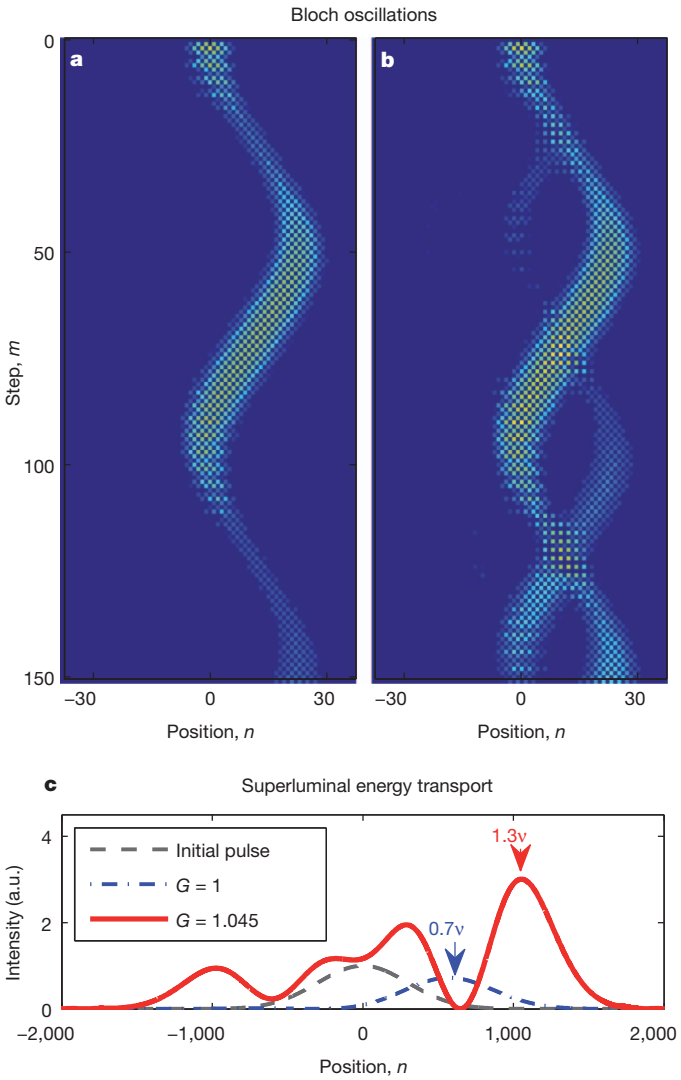

Figure 4 | Bloch oscillations (experiment) and superluminal energy transport (simulation). a, **b**, Bloch oscillations in the passive system (**a**) and in the system with gain/loss ($G = 1.08$) (**b**). A broad Gaussian input distribution is used to excite a narrow mode spectrum near the centre of the Brillouin zone. For each encounter with the imaginary parts of the band structure, a secondary light beam is emitted. A weak phase gradient $e^{i\alpha m}$ with $\alpha = \pi/25$ is applied to the long loop. Logarithmic colour scale: red, high intensity (1); dark blue, low intensity ($10^{-1.8}$). **c**, A broad initial pulse excitation with a narrow frequency spectrum close to the exceptional point speeds up the energy transport into the superluminal regime. The field distribution after $m = 800$ steps is shown for the passive case ($G = 1$) and the PT case ($G = 1.045$). Here v is the maximum possible speed of excitation spreading in the passive case (one step per round trip m). a.u., arbitrary units.

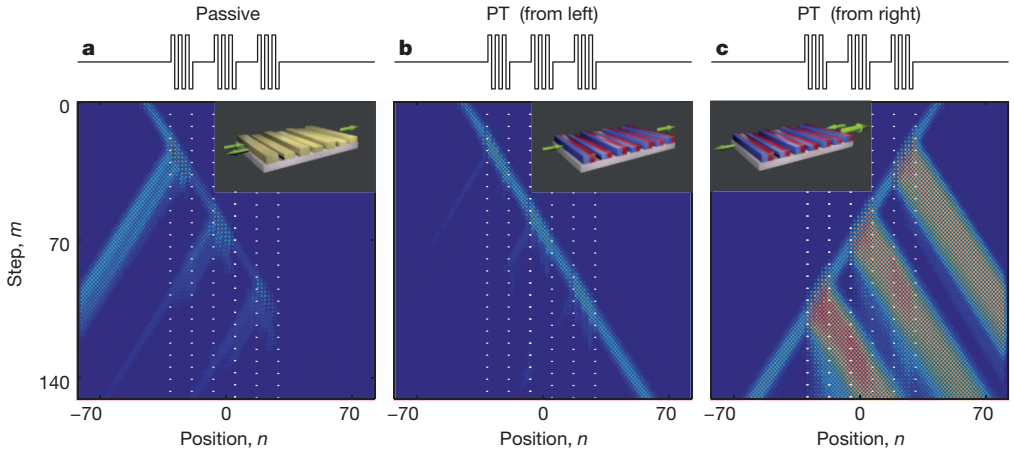

Figure 5 | Experimentally observed unidirectional invisibility of PT-symmetric Bragg scatterers. **a**, A broad pulse sequence is scattered off a series of passive Bragg elements ($2\varphi_0 = 0.36\pi$), which are implemented via phase modulation. **b**, Adding antisymmetric gain/loss ($G = 1.3$) at the positions of the scatterers puts the system at the PT threshold (PT). This renders the gratings invisible to a beam impinging from the left. **c**, If light comes from the right or, equivalently, gain and loss are exchanged, reflection is strongly enhanced while transmission remains unchanged. We note that the scatterers are again invisible for the newly generated reflections returning from the left. The positions of the three scatterers are indicated by vertical dotted lines. Logarithmic colour scale: red, high intensity (1); dark blue, low intensity (10^{-2}).

Pronounced outbursts of radiation are also observed when a broad input is subjected to a weak phase gradient in a PT-symmetric network above the symmetry-breaking point. As the beam dynamically changes its tilt, it performs Bloch oscillations[37–39] and sweeps the whole band structure (Fig. 4a, b). In this case, every time the field experiences imaginary eigenvalues, a secondary beam is emitted and the total power is amplified (Fig. 4b). Finally, the merging of the two bands at the exceptional points has even more intriguing consequences. Numerical simulations show that as the slope of the bands tends to infinity, the associated group velocity of a narrow-bandwidth wave packet increases and can even exceed the speed of light in the fibre[40] (without violating causality[41,42]), as indicated in Fig. 4c. This anomalous speed of the peak intensity is made possible by a gain-assisted growth of the distribution's leading tail. We note that all these features are a direct outcome of pseudo-hermiticity and have no analogue whatsoever in passive configurations.

Finally, we performed scattering experiments on a periodic, PT-symmetric temporal structure—a configuration analogous to a spatial grating (Fig. 5). As recently predicted[43,44], such structures have surprising behaviour such as unidirectional invisibility and unconventional reflection characteristics. More specifically, light propagating in such a system can experience reduced or enhanced reflections (with a coefficient that can even exceed one) depending on the direction of propagation. This is because left–right symmetry is broken in this PT network and propagation is no longer invariant when gain and loss are exchanged in time. Even more remarkable is what happens at the PT threshold: light waves entering the structure from one side do not experience any reflection and can fully traverse the grating with complete transmission. Given that this occurs without acquiring any phase imprint from the system, the periodic structure is essentially invisible[44]. However, if light is incident from the opposite side, the coefficient of reflection exceeds one. In our set-up, we created a temporal Bragg scatterer by imposing a periodic phase modulation $\varphi(n)$ only within a finite time window. Optical pulses travelling outside this window do not experience this periodic potential. In the absence of any gain or loss, the resulting passive configuration acts on incoming light as a reflector, very much like a spatial Bragg stack (Fig. 5a). Gain and loss was subsequently added to the phase modulation in a PT-symmetric fashion. Figure 5 shows experimental results confirming these predictions. Both suppression of reflection and full transmission exactly at the symmetry-breaking point are clearly observed, suggesting invisibility of the scatterers.

Our results demonstrate that scalable PT synthetic discrete systems can be realized using building blocks that respect this reflection symmetry. The modular approach presented here can be easily extended to on-chip configurations[45], thus paving the way for the realization of PT synthetic devices and effective media with new and unexpected optical properties. Finally, similar concepts can be effectively used in other areas such as plasmonics and metamaterials, where a harmonic coexistence of gain and loss is ultimately required. These and related issues are now accessible experimentally using the platform described here.

METHODS SUMMARY

Operation of the time-multiplexed fibre network in its passive version is described in ref. 33 and its supplementary information. To introduce gain and loss into the network, an acousto-optic modulator (AOM) was inserted into each loop. Both AOMs were operated in the zeroth order to implement a variable attenuation from 0 to 6 dB without imposing a frequency shift on the signal. The switching time of the AOMs was fast enough to change the attenuation between subsequent round trips (or between subsequent positions n in the case of PT scattering). The net gain of both loops provided by semiconductor optical amplifiers was varied so that the optical energy remained constant when the AOM losses were set to 3 dB. This allows the effective gain/loss to be modulated by up to ± 3 dB (that is, $G = 2$) in each loop.

The phase modulation for the potential was provided by an electro-optic phase modulator in the long loop. The imposed phase function used was

$$\varphi(n) = \begin{cases} -\varphi_0 & \text{for } \mathrm{mod}\,(n+3;4) = 0 \text{ or } 1 \\ +\varphi_0 & \text{for } \mathrm{mod}\,(n+3;4) = 2 \text{ or } 3 \end{cases}$$

To observe PT Bloch oscillations, the phase factor $e^{i\varphi(n)}$ in equation (1) was replaced by a linearly increasing phase gradient $e^{i\alpha m}$.

Only every second position n can be accessed by the optical pulses in our loop network. Therefore, the amplitudes in between are set to zero. The colour scales in Figs 2, 4 and 5 are logarithmic and are shown in Supplementary Figures 4, 5, 8 and 9. Further details concerning the experimental procedures followed can be found in Supplementary Methods.

Received 1 March; accepted 8 June 2012.

1. Joannopoulos, J. D., Villeneuve, P. R. & Fan, S. Photonic crystals: putting a new twist on light. *Nature* **386,** 143–149 (1997).
2. Knight, J. C., Broeng, J., Birks, T. A. & Russell, P. St J. Photonic band gap guidance in optical fibers. *Science* **282,** 1476–1478 (1998).
3. Barnes, W. L., Dereux, A. & Ebbesen, T. W. Surface plasmon subwavelength optics. *Nature* **424,** 824–830 (2003).
4. Stockman, M. Spaser action, loss compensation, and stability in plasmonic systems with gain. *Phys. Rev. Lett.* **106,** 156802 (2011).

5. Berini, P. & De Leon, I. Surface plasmon–polariton amplifiers and lasers. *Nature Photon.* **6,** 16–24 (2011).
6. Noginov, M. A. *et al.* Demonstration of a spaser-based nanolaser. *Nature* **460,** 1110–1112 (2009).
7. Pendry, J. B. Negative refraction makes a perfect lens. *Phys. Rev. Lett.* **85,** 3966–3969 (2000).
8. Bender, C. M. & Boettcher, S. Real spectra in non-Hermitian Hamiltonians having PT symmetry. *Phys. Rev. Lett.* **80,** 5243–5246 (1998).
9. Bender, C. M. Making sense of non-Hermitian Hamiltonians. *Rep. Prog. Phys.* **70,** 947–1018 (2007).
10. Lévai, G. & Znojil, M. Systematic search for PT-symmetric potentials with real energy spectra. *J. Phys. Math. Gen.* **33,** 7165–7180 (2000).
11. Bender, C. M., Brody, D. C. & Jones, H. F. Complex extension of quantum mechanics. *Phys. Rev. Lett.* **89,** 270401 (2002).
12. Mostafazadeh, A. Pseudo-Hermiticity versus PT symmetry: the necessary condition for the reality of the spectrum of a non-Hermitian Hamiltonian. *J. Math. Phys.* **43,** 205–214 (2002).
13. Berry, M. V. Optical lattices with PT symmetry are not transparent. *J. Phys. A* **41,** 244007 (2008).
14. Ahmed, Z. Real and complex discrete eigenvalues in an exactly solvable one-dimensional complex PT invariant potential. *Phys. Lett. A* **282,** 343–348 (2001).
15. Makris, K. G., El-Ganainy, R. & Christodoulides, D. N. Beam dynamics in PT symmetric optical lattices. *Phys. Rev. Lett.* **100,** 103904 (2008).
16. El-Ganainy, R., Makris, K. G., Christodoulides, D. N. & Musslimani, Z. H. Theory of coupled optical PT-symmetric structures. *Opt. Lett.* **32,** 2632–2634 (2007).
17. Makris, K. G., El-Ganainy, R. & Christodoulides, D. N. PT-symmetric optical lattices. *Phys. Rev. A* **81,** 063807 (2010).
18. Rüter, C. E. *et al.* Observation of parity–time symmetry in optics. *Nature Phys.* **6,** 192–195 (2010).
19. Guo, A. *et al.* Observation of PT-symmetry breaking in complex optical potentials. *Phys. Rev. Lett.* **103,** 093902 (2009).
20. Schindler, J., Li, A., Zheng, M. C., Ellis, F. M. & Kottos, T. Experimental study of active LRC circuits with PT symmetries. *Phys. Rev. A* **84,** 040101 (2011).
21. Bittner, S. *et al.* PT symmetry and spontaneous symmetry breaking in a microwave billiard. *Phys. Rev. Lett.* **108,** 024101 (2012).
22. Ramezani, H., Kottos, T., El-Ganainy, R. & Christodoulides, D. Unidirectional nonlinear PT-symmetric optical structures. *Phys. Rev. A* **82,** 043803 (2010) CrossRef.
23. Chong, Y., Ge, L. & Stone, A. PT-symmetry breaking and laser-absorber modes in optical scattering systems. *Phys. Rev. Lett.* **106,** 093902 (2011).
24. Klaiman, S., Guenther, U. & Moiseyev, N. Visualization of branch points in PT-symmetric waveguides. *Phys. Rev. Lett.* **101,** 080402 (2008).
25. Miroshnichenko, A. E., Malomed, B. A. & Kivshar, Y. S. Nonlinearly PT-symmetric systems: spontaneous symmetry breaking and transmission resonances. *Phys. Rev. A* **84,** 012123 (2011).
26. Suchkov, S. V. Dmitriev, S. V., Malomed, B. A. & Kivshar, Y. S. Wave scattering on a domain wall in a chain of PT-symmetric couplers. *Phys. Rev. A* **85,** 033825 (2012).
27. Uzdin, R. & Moiseyev, N. Scattering from a waveguide by cycling a non-Hermitian degeneracy. *Phys. Rev.* A **85,** 031804(R) (2012).
28. Kottos, T. Optical physics: broken symmetry makes light work. *Nature Phys.* **6,** 166–167 (2010).
29. Longhi, S. PT-symmetric laser absorber. *Phys. Rev. A* **82,** 031801(R) (2010).
30. Liertzer, M., Ge, L., Cerjan, A., Stone, A. D., Türeci, H. E., &. Rotter, S. Pump-induced exceptional points in lasers. *Phys. Rev. Lett.* **108,** 173901 (2012).
31. Miri, M.-A. LiKamWa, P. & Christodoulides, D. N. Large area single-mode parity–time-symmetric laser amplifiers. *Opt. Lett.* **37,** 764–766 (2012).
32. Schreiber, A. *et al.* Photons walking the line: a quantum walk with adjustable coin operations. *Phys. Rev. Lett.* **104,** 050502 (2010).
33. Regensburger, A. *et al.* Photon propagation in a discrete fiber network: an interplay of coherence and losses. *Phys. Rev. Lett.* **107,** 233902 (2011).
34. Zheng, M. C., Christodoulides, D. N., Fleischmann, R. & Kottos, T. PT optical lattices and universality in beam dynamics. *Phys. Rev.* A **82,** 010103(R) (2010).
35. Graefe, E. M. & Jones, H. F. PT-symmetric sinusoidal optical lattices at the symmetry-breaking threshold. *Phys. Rev. A* **84,** 013818 (2011).
36. Scott, D. D. & Joglekar, Y. N. Degrees and signatures of broken PT symmetry in nonuniform lattices. *Phys. Rev. A* **83,** 050102 (2011).
37. Longhi, S. Bloch oscillations in complex crystals with PT symmetry. *Phys. Rev. Lett.* **103,** 123601 (2009).
38. Pertsch, T., Dannberg, P., Elflein, W., Bräuer, A. & Lederer, F. Optical Bloch oscillations in temperature tuned waveguide arrays. *Phys. Rev. Lett.* **83,** 4752–4755 (1999).
39. Morandotti, R., Peschel, U., Aitchison, J., Eisenberg, H. & Silberberg, Y. Experimental observation of linear and nonlinear optical Bloch oscillations. *Phys. Rev. Lett.* **83,** 4756–4759 (1999).
40. Szameit, A., Rechtsman, M. C., Bahat-Treidel, O. & Segev, M. PT-symmetry in honeycomb photonic lattices. *Phys. Rev. A* **84,** 021806 (2011).
41. Chiao, R. Superluminal (but causal) propagation of wave-packets in transparent media with inverted atomic populations. *Phys. Rev. A* **48,** R34–R37 (1993).
42. Wang, L. J., Kuzmich, A. & Dogariu, A. Gain-assisted superluminal light propagation. *Nature* **406,** 277–279 (2000).
43. Kulishov, M., Laniel, J. M., Bélanger, N., Azaña, J. & Plant, D. V. Nonreciprocal waveguide Bragg gratings. *Opt. Express* **13,** 3068–3078 (2005).
44. Lin, Z. *et al.* Unidirectional invisibility induced by PT-symmetric periodic structures. *Phys. Rev. Lett.* **106,** 213901 (2011).
45. Sansoni, L. *et al.* Two-particle bosonic-fermionic quantum walk via integrated photonics. *Phys. Rev. Lett.* **108,** 010502 (2012).

Supplementary Information is linked to the online version of the paper at www.nature.com/nature.

Acknowledgements We acknowledge financial support from DFG Forschergruppe 760, the Cluster of Excellence Engineering of Advanced Materials, SAOT and the German-Israeli Foundation. This work was also supported by NSF grant ECCS-1128520 and by AFOSR grant FA95501210148. Moreover, we thank J. Näger for technical support.

Author Contributions All authors contributed extensively to the work presented in this paper.

Author Information Reprints and permissions information is available at www.nature.com/reprints. The authors declare no competing financial interests. Readers are welcome to comment on the online version of this article at www.nature.com/nature. Correspondence and requests for materials should be addressed to U.P. (ulf.peschel@physik.uni-erlangen.de) and D.N.C. (demetri@creol.ucf.edu).